PHYSICS

Giant nonlinear damping in nanoscale ferromagnets

I. Barsukov[1,2]*, H. K. Lee[1], A. A. Jara[1], Y.-J. Chen[1], A. M. Gonçalves[1], C. Sha[1], J. A. Katine[3], R. E. Arias[4], B. A. Ivanov[5,6], I. N. Krivorotov[1]

Magnetic damping is a key metric for emerging technologies based on magnetic nanoparticles, such as spin torque memory and high-resolution biomagnetic imaging. Despite its importance, understanding of magnetic dissipation in nanoscale ferromagnets remains elusive, and the damping is often treated as a phenomenological constant. Here, we report the discovery of a giant frequency-dependent nonlinear damping that strongly alters the response of a nanoscale ferromagnet to spin torque and microwave magnetic field. This damping mechanism originates from three-magnon scattering that is strongly enhanced by geometric confinement of magnons in the nanomagnet. We show that the giant nonlinear damping can invert the effect of spin torque on a nanomagnet, leading to an unexpected current-induced enhancement of damping by an antidamping torque. Our work advances the understanding of magnetic dynamics in nanoscale ferromagnets and spin torque devices.

INTRODUCTION

Nanoscale magnetic particles are the core components of several emerging technologies such as nonvolatile spin torque memory (*1*), spin torque oscillators (*2*–*7*), targeted drug delivery, and high-resolution biomagnetic imaging (*8*). Control of magnetic damping holds the key to improving the performance of many nanomagnet-based practical applications. In biomagnetic characterization techniques, such as magnetic resonance imaging, relaxometry, and magnetic particle imaging, magnetic damping affects nanoparticle relaxation times and image resolution. In spin torque memory and oscillators, magnetic damping determines the electrical current necessary for magnetic switching (*1*) and generation of auto-oscillations (*9*) and thereby determines energy efficiency of these technologies. The performance of nanomagnet-based microwave detectors is also directly affected by the damping (*10*–*12*). Despite its importance across multiple disciplines, magnetic damping in nanoparticles is poorly understood and is usually modeled as a phenomenological constant (*6*, *9*).

Here, we experimentally demonstrate that a ferromagnetic nanoparticle can exhibit dynamics qualitatively different from those predicted by the harmonic oscillator model. We show that nonlinear contributions to the damping can be unusually strong, and the effective damping parameter itself can exhibit resonant dependence on frequency. Our work demonstrates that nonlinear damping in nanomagnets is qualitatively different from that in bulk ferromagnets. We show both experimentally and theoretically that this nonlinear damping originates from multimagnon scattering in a magnetic system with a discrete spectrum of magnons induced by geometric confinement.

We also discover that the nonlinear damping markedly alters the response of a nanomagnet to spin torque. Spin torque arising from injection of spin currents polarized opposite to the direction of magnetization acts as negative damping (*2*). We find, however, that the effect of this antidamping spin torque is reversed, leading to an enhanced dissipation due to the nonlinear magnon scattering. This counterintuitive behavior should have substantial impact on the operation of spin torque–based memory (*1*), oscillators (*2*–*7*), and microwave detectors (*10*–*12*).

RESULTS

Spin wave spectroscopy

We study nonlinear spin wave dynamics in nanoscale elliptical magnetic tunnel junctions (MTJs) that consist of a CoFeB free layer (FL), an MgO tunnel barrier, and a synthetic antiferromagnet (SAF) pinned layer (*13*). Spectral properties of the FL spin wave modes are studied in a variety of MTJs with both in-plane and perpendicular-to-plane equilibrium orientations of the FL and SAF magnetization. We observe strong nonlinear damping in both the in-plane and the perpendicular MTJs, which points to the universality of the effect.

We use spin torque ferromagnetic resonance (ST-FMR) to measure magnetic damping of the FL spin wave modes. In this technique, a microwave drive current $I_{ac}\sin(2\pi ft)$ applied to the MTJ excites oscillations of magnetization at the drive frequency f. The resulting magnetoresistance oscillations $R_{ac}\sin(2\pi ft + \phi)$ generate a direct voltage V_{mix}. Peaks in ST-FMR spectra $V_{mix}(f)$ arise from resonant excitation of spin wave eigenmodes of the MTJ (*14*–*18*). To improve signal-to-noise ratio, the magnitude of external magnetic field H applied parallel to the FL magnetization is modulated, and a field-derivative signal $\tilde{V}_{mix}(f) = dV_{mix}(f)/dH$ is measured via lock-in detection technique (*13*). $V_{mix}(f)$ can then be obtained via numerical integration (note S1).

Figure 1A shows ST-FMR spectra $\tilde{V}_{mix}(f)$ measured as a function of out-of-plane magnetic field H for an elliptical 52 nm by 62 nm perpendicular MTJ device (sample 1). Three spin wave eigenmodes with nearly linear frequency–field relation $f_{n,m}(H)$ are visible in the spectra. Micromagnetic simulations (note S2) reveal that these modes are the three lowest frequency spin wave eigenmodes of the FL (fig. S1). The lowest frequency (quasi-uniform) mode $|0,0\rangle$ is nodeless and has spatially uniform phase. Each of the two higher-order modes $|n, m\rangle$ has a single node at the FL center that is either perpendicular $|0,1\rangle$ or parallel $|1,0\rangle$ to the ellipse long axis (Fig. 1B).

Although the spectra shown in Fig. 1A (especially for mode $|0,1\rangle$) strongly resemble avoided crossing, the physics giving rise to these spectral shapes is entirely different. An avoided crossing presumes two distinct modes, which eigenfrequencies would cross as a function of an external parameter (in our case, magnetic field) in the absence of mode interaction. In the variety of investigated MTJ samples, no such modes

[1]Physics and Astronomy, University of California, Irvine, CA 92697, USA. [2]Physics and Astronomy, University of California, Riverside, CA 92521, USA. [3]Western Digital, 5600 Great Oaks Parkway, San Jose, CA 95119, USA. [4]Departamento de Física, CEDENNA, FCFM, Universidad de Chile, Santiago, Chile. [5]Institute of Magnetism, National Academy of Sciences of Ukraine, Vernadsky Avenue 36B, Kyiv 03142, Ukraine. [6]National University of Science and Technology MISiS, Moscow 119049, Russian Federation.
*Corresponding author. Email: igorb@ucr.edu

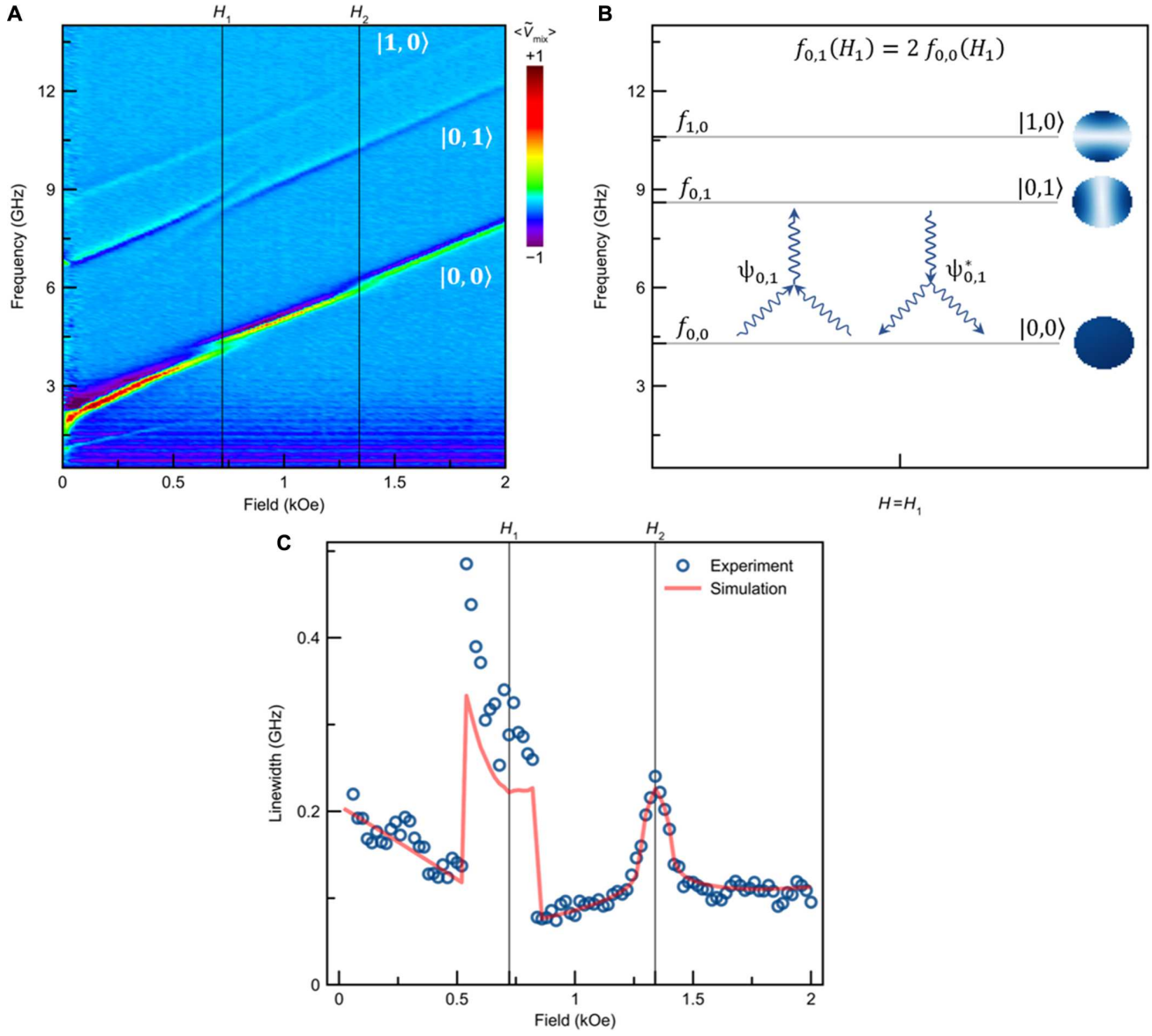

Fig. 1. Spin wave spectra in a nanoscale MTJ. (**A**) Normalized ST-FMR spectra $\langle\tilde{V}_{mix}(f)\rangle$ of spin wave eigenmodes in a perpendicular MTJ device (sample 1) measured as a function of out-of-plane magnetic field. Resonance peaks arising from three low frequency modes of the MTJ FL $|0,0\rangle$, $|0,1\rangle$, and $|1,0\rangle$ are observed. (**B**) Schematic of the three-magnon confluence process, denoted as $\psi_{0,1}$, and the inverse process of three-magnon splitting, denoted as $\psi^*_{0,1}$. Mode profiles are shown. (**C**) Spectral linewidth of the quasi-uniform $|0,0\rangle$ spin wave mode as a function of out-of-plane magnetic field. Strong linewidth enhancement is observed in the three-magnon scattering regime at H_1 and H_2.

exist. Neither spin wave modes localized in the FL nor SAF modes approach each other in energy as magnetic field is varied (Fig. 1A). Without these crossing modes, the observed lineshape irregularities of the three FL spin wave modes cannot be attributed to avoided crossing, and instead intrinsic nonlinearity of the system must be considered.

The spectral linewidth (Fig. 1C) of the resonances in Fig. 1A can be used for evaluation of the mode damping. The quasi-uniform mode $|0,0\rangle$ resonance visibly broadens at two magnetic field values: H_1 = 0.74 kOe (4 GHz) and H_2 = 1.34 kOe (6 GHz). Near H_1, the mode $|0,1\rangle$ resonance also broadens and exhibits splitting, the same behavior is observed for the mode $|1,0\rangle$ at H_2. At these fields, the higher-order mode frequency is twice that of the quasi-uniform mode $f_{n,m} = 2f_{0,0}$. This shows that three-magnon confluence (*19*–*24*) is the mechanism of the quasi-uniform mode damping increase (Fig. 1B): Two magnons of the quasi-uniform mode $|0,0\rangle$ merge into a single magnon of the higher-order mode $|n, m\rangle$.

The most notable feature of the quasi-uniform mode resonance near H_1 is its split-peak shape with a local minimum at the resonance frequency. Such a lineshape cannot be fit by the standard Lorentzian curve with symmetric and antisymmetric components (*13*). We therefore use a double-peak fitting function (note S1) to quantify the effective linewidth $\Delta f_{0,0}$ of the resonance profile. For applied fields sufficiently far from H_1, the ST-FMR curve recovers its single-peak shape, and $\Delta f_{0,0}$ is determined as half width of the standard Lorentzian fitting function (*13*). Figure 1C shows $\Delta f_{0,0}$ as a function of H and demonstrates a large increase of the linewidth near the fields of the

three-magnon scattering regime, H_1 and H_2. The stepwise increase of $\Delta f_{0,0}$ near H_1 is a result of the ST-FMR curve transition between the split-peak and single-peak shapes. For fields near H_2, the resonance profile broadens but does not develop a visible split-peak lineshape. As a result, $\Delta f_{0,0}(H)$ is a smooth function in the vicinity of H_2.

Effect of spin torque

In MTJs, direct bias current I_{dc} applied across the junction exerts spin torque on the FL magnetization, acting as antidamping for $I_{dc} > 0$ and as positive damping for $I_{dc} < 0$ (*15*, *25*). The antidamping spin torque increases the amplitude of the FL spin wave modes (*15*, *26*) and decreases their spectral linewidth (*27*). We can use spin torque from I_{dc} to control the amplitude of spin wave eigenmodes excited in ST-FMR measurements and thereby study the crossover between linear and nonlinear regimes of spin wave resonance. Increasing ac drive through the MTJ at zero direct current can also, in principle, be used to increase the spin wave amplitude and measure nonlinear damping. However, we found that this approach is not suitable for studying the linear-to-nonlinear transition because varying ac drive affects signal-to-noise ratio and often causes dielectric breakdown of the MgO barrier.

Figure 2 shows the dependence of ST-FMR resonance curve of the $|0,0\rangle$ mode $V_{mix}(f)$ on I_{dc} for a 50 nm by 110 nm elliptical in-plane MTJ (sample 2). For in-plane magnetic field values far from three-magnon scattering, the amplitude of ST-FMR resonance curve $V_{mix}(f)$ shown in Fig. 2A monotonically increases with increasing antidamping spin torque, as expected. At the three-magnon scattering field $H = H_1$, the antidamping spin torque has a radically different and rather unexpected effect on the resonance curve. As illustrated in Fig. 2C, increasing antidamping spin torque first broadens the resonance at $H = H_1$ and then transforms a single-peak resonance lineshape into a split-peak lineshape with a local minimum at the resonance frequency $f = f_{0,0}$. The data in Fig. 2 demonstrate that the unusual split-peak lineshape of the resonance is only observed when (i) the three-magnon scattering of the quasi-uniform mode is allowed by the conservation of energy and (ii) the amplitude of the mode is sufficiently high, confirming that the observed effect is resonant in the frequencies of two modes undergoing three-magnon scattering and nonlinear in nature.

Figure 2C reveals that antidamping spin torque can increase the spectral linewidth and the effective damping of the quasi-uniform spin mode if the mode undergoes three-magnon scattering. Figure 3 further illustrates this counterintuitive effect. It shows the linewidth of the quasi-uniform mode of a 50 nm by 110 nm elliptical in-plane MTJ (sample 3) measured as a function of bias current. In Fig. 3, blue open squares show the linewidth measured at an in-plane magnetic field sufficiently far from the three-magnon scattering. At this field, the expected quasi-linear dependence of the linewidth on I_{dc} is observed for currents well below the critical current for the excitation of auto-oscillatory magnetic dynamics. Near the critical current, the linewidth increases due to a combination of the fold-over effect (*28*, *29*) and thermally activated switching between the large- and small-amplitude oscillatory states of the fold-over regime (*15*). The red open circles in Fig. 3 show the linewidth measured in the three-magnon scattering regime at $H = H_1$. Here, in contrast, the linewidth increases with increasing $|I_{dc}|$ for both current polarities. Furthermore, the maximum linewidth is measured for the antidamping current polarity.

Theoretical model

Nonlinear interactions among spin wave eigenmodes of a ferromagnet give rise to a number of spectacular magnetodynamic phenomena such as Suhl instability of the uniform precession of magnetization (*30*, *31*), spin wave self-focusing (*32*), and magnetic soliton formation (*33*, *34*). In bulk ferromagnets, nonlinear interactions generally couple each spin wave eigenmode to a continuum of other modes via energy- and momentum-conserving multimagnon scattering (*30*). This kinematically allowed scattering limits the achievable amplitude of spin wave modes and leads to broadening of the spin wave resonance (*30*). It cannot explain the observed split-peak lineshape of the resonance. In nanoscale ferromagnets, geometric confinement discretizes the spin wave spectrum and thereby generally eliminates the kinematically

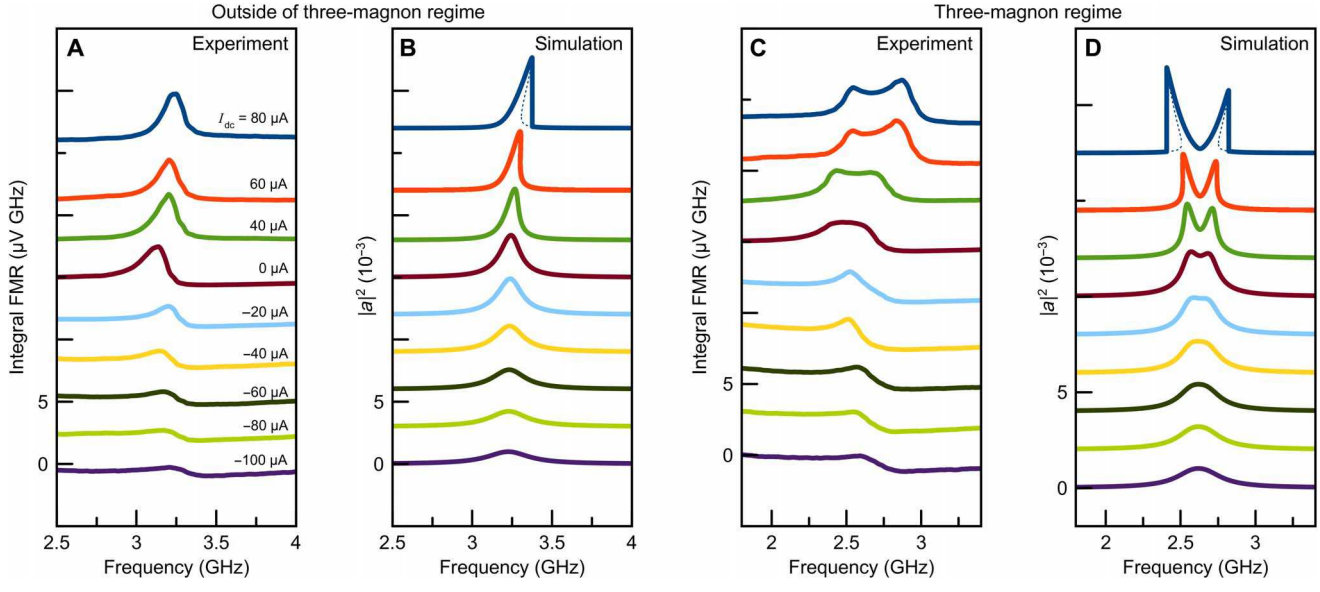

Fig. 2. Effect of spin torque on spin wave resonance lineshape. (**A** and **B**) Spin wave resonance lineshapes for different values of direct bias current I_{dc}, far from three-magnon scattering regime $H > H_1$. (**C** and **D**) Spin wave resonance lineshapes in the three-magnon regime at $H = H_1$. (A and C) Measured ST-FMR spectra (sample 2). (B and D) Solutions of Eqs. 3 and 4. Identical current values I_{dc}, displayed in (A), are used in all four figure panels.

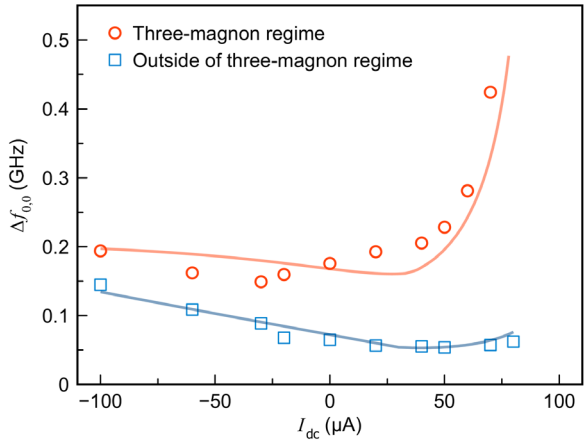

Fig. 3. Effect of spin torque on linewidth. Linewidth of the quasi-uniform spin wave mode as a function of applied direct bias current (sample 3): red open circles—in the three-magnon scattering regime $H = H_1$; blue open squares—far from the three-magnon scattering regime, $H \neq H_1$. Lines are numerical fits using Eqs. 3 and 4.

allowed multimagnon scattering. This suppression of nonlinear scattering enables persistent excitation of spin waves with very large amplitudes (*35*) as observed in nanomagnet-based spin torque oscillators (*2*). Tunability of the spin wave spectrum by external magnetic field, however, can lead to a restoration of the energy-conserving scattering (*21*). To describe the nonlinear spin wave resonance in the nanoscale ferromagnet and to derive the theory of nonlinear damping, we start with a model Hamiltonian that explicitly takes into account the nonlinear scattering between the quasi-uniform mode and a higher-order spin wave mode (in reduced units with $\hbar \equiv 1$)

$$\begin{aligned}\mathcal{H} &= \omega_{0,0}a^{\dagger}a + \omega_{n,m}b^{\dagger}b + \frac{\Psi_{0,0}}{2}a^{\dagger}a^{\dagger}aa + \frac{\Psi_{n,m}}{2}b^{\dagger}b^{\dagger}bb \\ &+(\psi_{n,m}aab^{\dagger} + \psi^{*}_{n,m}a^{\dagger}a^{\dagger}b) \\ &+\zeta\{\exp(-i\,\omega t)a^{\dagger} + \exp(i\,\omega t)a\}\end{aligned} \quad (1)$$

where $a^{\dagger}$, a and $b^{\dagger}$, b are the magnon creation and annihilation operators for the quasi-uniform mode $|0,0\rangle$ with frequency $\omega_{0,0}$ and for the higher-order spin wave mode $|n,m\rangle$ mode with frequency $\omega_{n,m}$, respectively. The nonlinear mode coupling term proportional to the coupling strength parameter $\psi_{n,m}$ describes the annihilation of two $|0,0\rangle$ magnons and creation of one $|n,m\rangle$ magnon, as well as the inverse process. The Hamiltonian is written in the resonant approximation, where small nonresonant terms such as aab and $aaa^{\dagger}$ are neglected. The terms proportional to $\Psi_{0,0}$ and $\Psi_{n,m}$ describe the intrinsic nonlinear frequency shifts (*36*) of the modes $|0,0\rangle$ and $|n,m\rangle$. The last term describes the excitation of the quasi-uniform mode by an external ac drive with the amplitude ζ and frequency ω.

We further define classically a dissipation function Q, where $\alpha_{0,0}$ and $\alpha_{n,m}$ are the intrinsic linear damping parameters of the modes $|0,0\rangle$ and $|n,m\rangle$ (*37*)

$$Q = \frac{da^{\dagger}}{dt}\frac{da}{dt}(\alpha_{0,0} + \eta_{0,0}a^{\dagger}a) + \frac{db^{\dagger}}{dt}\frac{db}{dt}(\alpha_{n,m} + \eta_{n,m}b^{\dagger}b) \quad (2)$$

For generality, Eq. 2 includes intrinsic nonlinear damping (*9*) of the modes $|0,0\rangle$ and $|n,m\rangle$ described by the nonlinearity parameters $\eta_{0,0}$ and $\eta_{n,m}$. However, our analysis below shows that the split-peak resonance lineshape is predicted by our theory even if $\eta_{0,0}$ and $\eta_{n,m}$ are set equal to zero.

Equations describing the nonlinear dynamics of the two coupled spin wave modes of the system follow from Eqs. 1 and 2 via

$$i\frac{da}{dt} = \frac{\partial\mathcal{H}}{\partial a^{\dagger}} + \frac{\partial Q}{\partial(da^{\dagger}/dt)} \quad (3)$$

$$i\frac{db}{dt} = \frac{\partial\mathcal{H}}{\partial b^{\dagger}} + \frac{\partial Q}{\partial(db^{\dagger}/dt)} \quad (4)$$

It can be shown (note S3) that these equations have a periodic solution $a = \bar{a}\exp(-i\,\omega t)$ and $b = \bar{b}\exp(-i\,2\omega t)$, where $\bar{a}$ and $\bar{b}$ are the complex spin wave mode amplitudes. For this periodic solution, Eqs. 3 and 4 are reduced to a set of two nonlinear algebraic equations for absolute values of the spin wave mode amplitudes $|\bar{a}|$ and $|\bar{b}|$, which can be solved numerically. Since the ST-FMR signal is proportional to $|\bar{a}|^2$ (note S1), the calculated $|\bar{a}|^2(\omega)$ function can be directly compared to the measured ST-FMR resonance lineshape.

We use the solution of Eqs. 3 and 4 to fit the field dependence of the quasi-uniform mode linewidth in Fig. 1C. In this fitting procedure, the resonance lineshape $|\bar{a}|^2(\omega)$ is calculated, and its spectral linewidth $\Delta\omega_{0,0}$ is found numerically. The resonance frequencies $\omega_{0,0}$ and $\omega_{n,m}$ are directly determined from the ST-FMR data in Fig. 1A. The intrinsic damping parameters $\alpha_{0,0}$ and $\alpha_{n,m}$ near H_1 and H_2 are found from linear interpolations of the ST-FMR linewidths $\Delta f_{0,0}$ and $\Delta f_{n,m}$ measured at fields far from H_1 and H_2. We find that $\Delta\omega_{0,0}$ weakly depends on the nonlinearity parameters Ψ and η, and thus, these parameters are set to zero (fig. S2). We also find that the calculated linewidth $\Delta\omega_{0,0}$ depends on the product of the drive amplitude ζ and mode coupling strength $\psi_{n,m}$ but is nearly insensitive to the individual values of ζ and $\psi_{n,m}$ as long as $\zeta \cdot \psi_{n,m}$ = const (fig. S3 and note S4). Therefore, we use $\zeta \cdot \psi_{n,m}$ as a single fitting parameter in this fitting procedure. The solid line in Fig. 1C shows the calculated field dependence of the quasi-uniform mode linewidth on magnetic field. The agreement of this single-parameter fit with the experiment is excellent.

Fig. 2 (B and D) illustrates that Eqs. 3 and 4 not only describe the field dependence of ST-FMR linewidth but also qualitatively reproduce the spectral lineshapes of the measured ST-FMR resonances and the effect of the antidamping spin torque on the lineshapes. Figure 2B shows the dependence of the calculated lineshape $|\bar{a}|^2(\omega)$ on antidamping spin torque for a magnetic field H far from the three-magnon scattering fields. Here, the increasing antidamping spin torque induces the fold-over of the resonance curve (*28*) without resonance peak splitting. The dependence of $|\bar{a}|^2(\omega)$ on antidamping spin torque for $H = H_1$ is shown in Fig. 2D. At this field, the resonance peak in $|\bar{a}|^2(\omega)$ first broadens with increasing antidamping spin torque and then splits, in qualitative agreement with the experimental ST-FMR data in Fig. 2C. Our calculations (fig. S2) reveal that while the nonlinearity parameters $\Psi_{0,0}$, $\eta_{0,0}$, $\Psi_{n,m}$, and $\eta_{n,m}$ have little effect on the linewidth $\Delta\omega_{0,0}$, they modify the lineshape of the resonance. Given that the nonlinearity parameter values are not well known for the systems studied here, we do not attempt to quantitatively fit the measured ST-FMR lineshapes.

Equations 3 and 4 also quantitatively explain the observed dependence of the quasi-uniform mode linewidth $\Delta\omega_{0,0}$ on direct bias current I_{dc}. Assuming antidamping spin torque linear in bias current (*27*, *38*, *39*), $\alpha_{0,0} \rightarrow \alpha_{0,0}(1 - I_{dc}/I_c^{|0,0\rangle})$, $\alpha_{n,m} \rightarrow \alpha_{n,m}(1 - I_{dc}/I_c^{|n,m\rangle})$, where $I_c^{|n,m\rangle} > I_c^{|0,0\rangle}$ are the critical currents, we fit the measured bias dependence of ST-FMR linewidth in Fig. 3 by solving Eqs. 3 and 4. The solid lines in Fig. 3 are the best numerical fits, where $\zeta \cdot \psi_{n,m}$ and I_c are used as independent fitting parameters. The rest of the parameters in Eqs. 3 and 4 are directly determined from the experiment, following the procedure used for fitting the data in Fig. 1C. Theoretical curves in Fig. 3 capture the main feature of the data at the three-magnon scattering field H_1, which is an increase of the linewidth with increasing antidamping spin torque.

DISCUSSION

Quantitative understanding of the mechanisms of the nonlinear spin wave resonance peak splitting and broadening by antidamping spin torque can be gained by neglecting the intrinsic nonlinearities $\Psi_{n,m}$ and $\eta_{n,m}$ of the higher-order mode $|n,m\rangle$. Setting $\Psi_{n,m} = 0$ and $\eta_{n,m} = 0$ in Eqs. 3 and 4 allows us to reduce the equation of motion for the quasi-uniform mode amplitude $|\bar{a}|$ to the standard equation for a single-mode damped driven oscillator (notes S5 and S6), where a constant damping parameter $\alpha_{0,0}$ is replaced by an effective frequency-dependent nonlinear damping parameter $\alpha_{0,0}^{eff}$

$$\alpha_{0,0}^{eff} = \alpha_{0,0} + \left[\eta_{0,0} + \frac{4\alpha_{n,m}\psi_{n,m}^2}{(2\omega - \omega_{n,m})^2 + 4\alpha_{n,m}^2\omega^2}\right]|\bar{a}|^2 \quad (5)$$

and the resonance frequency is replaced by an effective resonance frequency

$$\omega_{0,0}^{eff} = \omega_{0,0} + \left[\Psi_{0,0} + \frac{2|\psi_{n,m}|^2(2\omega - \omega_{n,m})}{(2\omega - \omega_{n,m})^2 + 4\alpha_{n,m}^2\omega^2}\right]|\bar{a}|^2 \quad (6)$$

Equation 5 shows that the damping parameter of the quasi-uniform mode itself becomes a resonant function of the drive frequency with a maximum at half the frequency of the higher-order mode ($\omega = \frac{1}{2}\omega_{n,m}$). The amplitude and the width of this resonant behavior of $\alpha_{0,0}^{eff}(\omega)$ are determined by the intrinsic damping parameter $\alpha_{n,m}$ of the higher-order mode $|n,m\rangle$. If $\alpha_{n,m}$ is sufficiently small, the quasi-uniform mode damping is strongly enhanced at $\omega = \frac{1}{2}\omega_{n,m}$, which leads to a decrease of the quasi-uniform mode amplitude at this drive frequency. If the drive frequency is shifted away from $\frac{1}{2}\omega_{n,m}$ to either higher or lower values, the damping decreases, which can result in an increase of the quasi-uniform mode amplitude $|\bar{a}|$. Therefore, the amplitude of the quasi-uniform mode $|\bar{a}|(\omega)$ can exhibit a local minimum at $\omega = \frac{1}{2}\omega_{n,m}$. Because of its nonlinear origin, the tendency to form a local minimum in $|\bar{a}|(\omega)$ at $\frac{1}{2}\omega_{n,m}$ is enhanced with increasing $|\bar{a}|$. Since $|\bar{a}|$ is large near the resonance frequency $\omega_{0,0}$, tuning $\omega_{0,0}$ to be equal to $\frac{1}{2}\omega_{n,m}$ greatly amplifies the effect of local minimum formation in $|\bar{a}|(\omega)$. This qualitative argument based on Eq. 5 explains the data in Fig. 2—the split-peak nonlinear resonance of the quasi-uniform mode is only observed when external magnetic field tunes the spin wave eigenmode frequencies to the three-magnon scattering condition $\omega_{0,0} = \frac{1}{2}\omega_{n,m}$.

Equation 6 reveals that the nonlinear frequency shift of the quasi-uniform mode also presents a resonant behavior with respect to the drive frequency. In contrast to the nonlinear damping resonance described by Eq. 5, the frequency shift is an antisymmetric function of $(\omega - \frac{1}{2}\omega_{n,m})$. The nonlinear shift is negative for $\omega < \frac{1}{2}\omega_{n,m}$ and thus causes a fold-over toward lower frequencies, while it is positive for $\omega > \frac{1}{2}\omega_{n,m}$, causing fold-over toward higher frequencies. At the center of the resonance profile, the three-magnon process induces no frequency shift. This double-sided fold-over also contributes to the formation of the split-peak lineshape of the resonance shown in Fig. 2 (C and D) and to the linewidth broadening. As with the nonlinear damping enhancement, the antisymmetric nonlinear frequency shift and the double-sided fold-over become greatly amplified when the spin wave mode frequencies are tuned near the three-magnon scattering $\omega_{0,0} = \frac{1}{2}\omega_{n,m}$. Note that the mode $|0,1\rangle$ at the three-magnon scattering field $H = H_1$ in Fig. 1A presents a qualitatively similar split-peak profile. When the MTJ is driven by microwave at frequencies near $f = f_{0,1}$, the mode $|0,1\rangle$ decays into the $|0,0\rangle$ mode via three-magnon splitting process. Because of the discrete spectrum of magnons, the effective damping of the spin wave modes $|n,m\rangle$ presents a resonant character as well.

Equations 5 and 6 also shed light on the origin of the quasi-uniform mode line broadening by the antidamping spin torque. The antidamping spin torque increases the quasi-uniform mode amplitude $|\bar{a}|$ via transfer of angular momentum from spin current to the mode. Since the nonlinear damping and the nonlinear frequency shift are both proportional to $|\bar{a}|^2$ and both contribute to the line broadening, the antidamping spin torque can indeed give rise to the line broadening. Equation 5 reveals two competing effects of the antidamping spin torque on the quasi-uniform mode damping parameter $\alpha_{0,0}^{eff}$: Spin torque from I_{dc} decreases the linear component of the damping parameter $\alpha_{0,0} \rightarrow \alpha_{0,0}(1 - I_{dc}/I_c^{|0,0\rangle})$ and increases the nonlinear component via increased $|\bar{a}|^2$. Whether the antidamping spin torque decreases or increases the spectral linewidth of the mode depends on the system parameters. Our numerical solution of Eqs. 3 and 4 shown in Fig. 3 demonstrates that the antidamping spin torque can strongly increase the linewidth of the quasi-uniform mode when the three-magnon scattering condition $\omega_{0,0} = \frac{1}{2}\omega_{n,m}$ is satisfied.

Here, we find that the three-magnon processes in strongly confined magnets are cardinally different from multimagnon processes known in bulk (*19*, *30*). A prominent example of three-magnon processes in bulk systems is Suhl instability, where a magnon of uniform precession decays in two magnons of nonuniform precession. In our case, we observe an inverse process, where two uniform magnons merge into one nonuniform magnon. This process (*24*) does not exhibit a threshold behavior characteristic for Suhl instabilities; we find no threshold behavior upon increasing amplitude (fig. S2) or decreasing intrinsic damping. Yet, there is another fundamental difference of the three-magnon process studied here from multimagnon processes in bulk ferromagnets. In a nanomagnet, translational invariance is broken. The three-magnon processes thus require only conservation of energy, as opposed to extended systems with continuous magnon spectra where momentum must be conserved as well. The three-magnon process in an extended system is described by $\omega(0) = \omega(\vec{k}) + \omega(-\vec{k})$. The three-magnon process studied here is not allowed in extended systems, where it would require merging of two $k = 0$ (uniform mode) magnons into a magnon with $k \neq 0$, which violates conservation of momentum. The pronounced resonant character (*40*) of the

nonlinearity (resonant behavior with respect to the frequencies of the modes undergoing three-magnon scattering), the split-peak spectra, and the inversion of the antidamping effect are thus unique to confined systems such as nanomagnets.

We expect that the nonlinear damping discovered in this work will have strong impact on the performance of spin torque devices such as spin torque magnetic memory, spin torque nano-oscillators, and spin torque microwave detectors. Since all these devices rely on large-amplitude oscillations of magnetization driven by spin torque, the amplitude limiting resulting from the nonlinear damping is expected to have detrimental effect on the device performance.

In conclusion, our measurements demonstrate that magnetic damping of spin wave modes in a nanoscale ferromagnet has a strong nonlinear component of resonant character that appears at a discrete set of magnetic fields corresponding to three-magnon scattering. This nonlinearity can give rise to unusual spin wave resonance profiles with a local minimum at the resonance frequency in sharp contrast to the properties of the linear and nonlinear spin wave resonances in bulk ferromagnets. The nonlinearity has a profound effect on the response of the nanomagnet to spin torque. Antidamping spin torque, which reduces the quasi-uniform spin wave mode damping at magnetic fields far from the three-magnon scattering regime, can enhance the damping in the scattering regime. This inversion of the effect of spin torque on magnetization dynamics is expected to have substantial impact on the performance of nanoscale spin torque devices such as magnetic memory and spin torque oscillators.

SUPPLEMENTARY MATERIALS

Supplementary material for this article is available at http://advances.sciencemag.org/cgi/content/full/5/10/eaav6943/DC1

Note S1. Calculation of linewidth.
Note S2. Micromagnetic simulations.
Note S3. Solution of the equations of motion.
Note S4. Effect of the drive amplitude and intrinsic nonlinearitites on the resonance lineshape.
Note S5. Effective single-mode nonlinear oscillator approximation.
Note S6. Mode coupling parameter.
Fig. S1. Spatial profiles of spin wave eigenmodes.
Fig. S2. Effect of intrinsic nonlinearities on the quasi-uniform spin wave resonance lineshape.
Fig. S3. Effect of the drive amplitude on linewidth in the three-magnon regime.
References (*41*–*47*)

REFERENCES AND NOTES

1. L. Liu, C.-F. Pai, Y. Li, H. W. Tseng, D. C. Ralph, R. A. Buhrman, Spin-torque switching with the giant spin Hall effect of tantalum. *Science* **336**, 555–558 (2012).
2. S. I. Kiselev, J. C. Sankey, I. N. Krivorotov, N. C. Emley, R. J. Schoelkopf, R. A. Buhrman, D. C. Ralph, Microwave oscillations of a nanomagnet driven by a spin-polarized current. *Nature* **425**, 380–383 (2003).
3. W. H. Rippard, A. M. Deac, M. R. Pufall, J. M. Shaw, M. W. Keller, S. E. Russek, G. E. W. Bauer, C. Serpico, Spin-transfer dynamics in spin valves with out-of-plane magnetized CoNi free layers. *Phys. Rev. B* **81**, 014426 (2010).
4. D. Houssameddine, U. Ebels, B. Delaët, B. Rodmacq, I. Firastrau, F. Ponthenier, M. Brunet, C. Thirion, J.-P. Michel, L. Prejbeanu-Buda, M.-C. Cyrille, O. Redon, B. Dieny, Spin-torque oscillator using a perpendicular polarizer and a planar free layer. *Nat. Mater.* **6**, 447–453 (2007).
5. A. Houshang, E. Iacocca, P. Dürrenfeld, S. R. Sani, J. Åkerman, R. K. Dumas, Spin-wave-beam driven synchronization of nanocontact spin-torque oscillators. *Nat. Nanotechnol.* **11**, 280–286 (2016).
6. V. E. Demidov, S. Urazhdin, H. Ulrichs, V. Tiberkevich, A. Slavin, D. Baither, G. Schmitz, S. O. Demokritov, Magnetic nano-oscillator driven by pure spin current. *Nat. Mater.* **11**, 1028–1031 (2012).
7. F. Macià, D. Backes, A. D. Kent, Stable magnetic droplet solitons in spin-transfer nanocontacts. *Nat. Nanotechnol.* **9**, 992–996 (2014).
8. Z. Cheng, A. Al Zaki, J. Z. Hui, V. R. Muzykantov, A. Tsourkas, Multifunctional nanoparticles: Cost versus benefit of adding targeting and imaging capabilities. *Science* **338**, 903–910 (2012).
9. A. Slavin, V. Tiberkevich, Nonlinear auto-oscillator theory of microwave generation by spin-polarized current. *IEEE Trans. Magn.* **45**, 1875–1918 (2009).
10. J. Zhu, J. A. Katine, G. E. Rowlands, Y.-J. Chen, Z. Duan, J. G. Alzate, P. Upadhyaya, J. Langer, P. K. Amiri, K. L. Wang, I. N. Krivorotov, Voltage-induced ferromagnetic resonance in magnetic tunnel junctions. *Phys. Rev. Lett.* **108**, 197203 (2012).
11. S. Miwa, S. Ishibashi, H. Tomita, T. Nozaki, E. Tamura, K. Ando, N. Mizuochi, T. Saruya, H. Kubota, K. Yakushiji, T. Taniguchi, H. Imamura, A. Fukushima, S. Yuasa, Y. Suzuki, Highly sensitive nanoscale spin-torque diode. *Nat. Mater.* **13**, 50–56 (2014).
12. B. Fang, M. Carpentieri, X. Hao, H. Jiang, J. A. Katine, I. N. Krivorotov, B. Ocker, J. Langer, K. L. Wang, B. Zhang, B. Azzerboni, P. K. Amiri, G. Finocchio, Z. Zeng, Giant spin-torque diode sensitivity in the absence of bias magnetic field. *Nat. Commun.* **7**, 11259 (2016).
13. A. M. Gonçalves, I. Barsukov, Y.-J. Chen, L. Yang, J. A. Katine, I. N. Krivorotov, Spin torque ferromagnetic resonance with magnetic field modulation. *Appl. Phys. Lett.* **103**, 172406 (2013).
14. A. A. Tulapurkar, Y. Suzuki, A. Fukushima, H. Kubota, H. Maehara, K. Tsunekawa, D. D. Djayaprawira, N. Watanabe, S. Yuasa, Spin-torque diode effect in magnetic tunnel junctions. *Nature* **438**, 339–342 (2005).
15. J. C. Sankey, P. M. Braganca, A. G. F. Garcia, I. N. Krivorotov, R. A. Buhrman, D. C. Ralph, Spin-transfer-driven ferromagnetic resonance of individual nanomagnets. *Phys. Rev. Lett.* **96**, 227601 (2006).
16. M. Shinozaki, E. Hirayama, S. Kanai, H. Sato, F. Matsukura, H. Ohno, Damping constant in a free layer in nanoscale CoFeB/MgO magnetic tunnel junctions investigated by homodyne-detected ferromagnetic resonance. *Appl. Phys. Exp.* **10**, 013001 (2017).
17. C. J. Safranski, Y.-J. Chen, I. N. Krivorotov, J. Z. Sun, Material parameters of perpendicularly magnetized tunnel junctions from spin torque ferromagnetic resonance techniques. *Appl. Phys. Lett.* **109**, 132408 (2016).
18. O. Mosendz, J. E. Pearson, F. Y. Fradin, G. E. W. Bauer, S. D. Bader, A. Hoffmann, Quantifying spin Hall angles from spin pumping: Experiments and theory. *Phys. Rev. Lett.* **104**, 046601 (2010).
19. C. L. Ordóñez-Romero, B. A. Kalinikos, P. Krivosik, W. Tong, P. Kabos, C. E. Patton, Three-magnon splitting and confluence processes for spin-wave excitations in yttrium iron garnet films: Wave vector selective Brillouin light scattering measurements and analysis. *Phys. Rev. B* **79**, 144428 (2009).
20. H. Schultheiss, X. Janssens, M. van Kampen, F. Ciubotaru, S. J. Hermsdoerfer, B. Obry, A. Laraoui, A. A. Serga, L. Lagae, A. N. Slavin, B. Leven, B. Hillebrands, Direct current control of three magnon scattering processes in spin-valve nanocontacts. *Phys. Rev. Lett.* **103**, 157202 (2009).
21. C. T. Boone, J. A. Katine, J. R. Childress, V. Tiberkevich, A. Slavin, J. Zhu, X. Cheng, I. N. Krivorotov, Resonant nonlinear damping of quantized spin waves in ferromagnetic nanowires: A spin torque ferromagnetic resonance study. *Phys. Rev. Lett.* **103**, 167601 (2009).
22. H. Kurebayashi, O. Dzyapko, V. E. Demidov, D. Fang, A. J. Ferguson, S. O. Demokritov, Controlled enhancement of spin-current emission by three-magnon splitting. *Nat. Mater.* **10**, 660–664 (2011).
23. R. N. Costa Filho, M. G. Cottam, G. A. Farias, Microscopic theory of dipole-exchange spin waves in ferromagnetic films: Linear and nonlinear processes. *Phys. Rev. B* **62**, 6545–6560 (2000).
24. V. E. Demidov, M. P. Kostylev, K. Rott, P. Krzysteczko, G. Reiss, S. O. Demokritov, Generation of the second harmonic by spin waves propagating in microscopic stripes. *Phys. Rev. B* **83**, 054408 (2011).
25. A. M. Deac, A. Fukushima, H. Kubota, H. Maehara, Y. Suzuki, S. Yuasa, Y. Nagamine, K. Tsunekawa, D. D. Djayaprawira, N. Watanabe, Bias-driven high-power microwave emission from MgO-based tunnel magnetoresistance devices. *Nat. Phys.* **4**, 803–809 (2008).
26. V. E. Demidov, S. Urazhdin, E. R. J. Edwards, M. D. Stiles, R. D. McMichael, S. O. Demokritov, Control of magnetic fluctuations by spin current. *Phys. Rev. Lett.* **107**, 107204 (2011).
27. G. D. Fuchs, J. C. Sankey, V. S. Pribiag, L. Qian, P. M. Braganca, A. G. F. Garcia, E. M. Ryan, Z.-P. Li, O. Ozatay, D. C. Ralph, R. A. Buhrman, Spin-torque ferromagnetic resonance measurements of damping in nanomagnets. *Appl. Phys. Lett.* **91**, 062507 (2007).
28. G. A. Melkov, D. V. Slobodianiuk, V. S. Tiberkevich, G. de Loubens, O. Klein, A. N. Slavin, Nonlinear ferromagnetic resonance in nanostructures having discrete spectrum of spin-wave modes. *IEEE Magn. Lett.* **4**, 4000504 (2013).
29. J. Podbielski, D. Heitmann, D. Grundler, Microwave-assisted switching of microscopic rings: Correlation between nonlinear spin dynamics and critical microwave fields. *Phys. Rev. Lett.* **99**, 207202 (2007).
30. H. Suhl, The theory of ferromagnetic resonance at high signal powers. *J. Phys. Chem. Solid* **1**, 209–227 (1957).
31. H. G. Bauer, P. Majchrak, T. Kachel, C. H. Back, G. Woltersdorf, Nonlinear spin-wave excitations at low magnetic bias fields. *Nat. Commun.* **6**, 8274 (2015).

32. M. Bauer, O. Büttner, S. O. Demokritov, B. Hillebrands, V. Grimalsky, Y. Rapoport, A. N. Slavin, Observation of spatiotemporal self-focusing of spin waves in magnetic films. *Phys. Rev. Lett.* **81**, 3769–3772 (1998).
33. A. M. Kosevich, B. A. Ivanov, A. S. Kovalev, Magnetic solitons. *Phys. Rep.* **194**, 117–238 (1990).
34. M. Wu, B. A. Kalinikos, C. E. Patton, Self-generation of chaotic solitary spin wave pulses in magnetic film active feedback rings. *Phys. Rev. Lett.* **95**, 237202 (2005).
35. M. d'Aquino, A. Quercia, V. Scalera, S. Perna, G. Bertotti, I. D. Mayergoyz, C. Serpico, Analytical treatment of nonlinear ferromagnetic resonance in nanomagnets. *IEEE Trans. Magn.* **53**, 4301005 (2017).
36. F. Guo, L. M. Belova, R. D. McMichael, Nonlinear ferromagnetic resonance shift in submicron permalloy ellipses. *Phys. Rev. B* **91**, 064426 (2015).
37. H. T. Nembach, J. M. Shaw, C. T. Boone, T. J. Silva, Mode- and size-dependent Landau-Lifshitz damping in magnetic nanostructures: Evidence for nonlocal damping. *Phys. Rev. Lett.* **110**, 117201 (2013).
38. V. Lauer, D. A. Bozhko, T. Brächer, P. Pirro, V. I. Vasyuchka, A. A. Serga, M. B. Jungfleisch, M. Agrawal, Y. V. Kobljanskyj, G. A. Melkov, C. Dubs, B. Hillebrands, A. V. Chumak, Spin-transfer torque based damping control of parametrically excited spin waves in a magnetic insulator. *Appl. Phys. Lett.* **108**, 012402 (2016).
39. C. Zhang, Y. Pu, S. A. Manuilov, S. P. White, M. R. Page, E. C. Blomberg, D. V. Pelekhov, P. C. Hammel, Engineering the spectrum of dipole field-localized spin-wave modes to enable spin-torque antidamping. *Phys. Rev. Appl.* **7**, 054019 (2017).
40. O. Shoshani, S. W. Shaw, M. I. Dykman, Anomalous decay of nanomechanical modes going through nonlinear resonance. *Sci. Rep.* **7**, 18091 (2017).
41. M. Harder, Y. Gui, C.-M. Hu, Electrical detection of magnetization dynamics via spin rectification effects. *Phys. Rep.* **661**, 1–59 (2016).
42. M. J. Donahue, D. G. Porter, *OOMMF User's Guide* (National Institute of Standards and Technology, 1999).
43. R. D. McMichael, M. D. Stiles, Magnetic normal modes of nanoelements. *J. Appl. Phys.* **97**, 10J901 (2005).
44. P. S. Keatley, V. V. Kruglyak, A. Neudert, R. J. Hicken, V. D. Poimanov, J. R. Childress, J. A. Katine, Resonant enhancement of damping within the free layer of a microscale magnetic tunnel valve. *J. Appl. Phys.* **117**, 17B301 (2015).
45. T. Holstein, H. Primakoff, Field dependence of the intrinsic domain magnetization of a ferromagnet. *Phys. Rev.* **58**, 1098–1113 (1940).
46. D. Mancilla-Almonacid, R. E. Arias, Instabilities of spin torque driven auto-oscillations of a ferromagnetic disk magnetized in plane. *Phys. Rev. B* **93**, 224416 (2016).
47. D. Mancilla-Almonacid, R. E. Arias, Spin-wave modes in ferromagnetic nanodisks, their excitation via alternating currents and fields, and auto-oscillations. *Phys. Rev. B* **95**, 214424 (2017).

Acknowledgments

Funding: This work was supported by the National Science Foundation through grants nos. DMR-1610146, EFMA-1641989, ECCS-1708885, and ECCS-1810541. We also acknowledge support by the Army Research Office through grant no. W911NF-16-1-0472 and Defense Threat Reduction Agency through grant no. HDTRA1-16-1-0025. A.M.G. thanks CAPES Foundation, Ministry of Education of Brazil for financial support. R.E.A. acknowledges Financiamiento Basal para Centros Cientificos y Tecnologicos de Excelencia under project FB 0807 (Chile) and Grant ICM P10-061-F by Fondo de Innovacion para la Competitividad-MINECON. B.A.I. was supported by the National Academy of Sciences of Ukraine via project no. 1/17-N and by the Program of NUST "MISIS" (grant no. K2-2017-005), implemented by a governmental decree dated 16 March 2013, no. 211. **Author contributions:** I.B. designed experiments, performed measurements, and carried out numerical calculations. H.K.L. and A.M.G. performed measurements. J.A.K. made the samples. Y.-J.C. and C.S. performed micromagnetic simulations. A.A.J. carried out numerical calculations. R.E.A. developed a model for the spin wave coupling parameter. B.A.I. developed the nonlinear theory. I.N.K. managed the project. All authors analyzed the data and co-wrote the paper. **Competing interests:** The authors declare that they have no competing interests. **Data and materials availability:** All data needed to evaluate the conclusions in the paper are present in the paper and/or the Supplementary Materials. Additional data related to this paper may be requested from the authors.

Submitted 24 January 2019
Accepted 13 September 2019
Published 25 October 2019
10.1126/sciadv.aav6943

Citation: I. Barsukov, H. K. Lee, A. A. Jara, Y.-J. Chen, A. M. Gonçalves, C. Sha, J. A. Katine, R. E. Arias, B. A. Ivanov, I. N. Krivorotov, Giant nonlinear damping in nanoscale ferromagnets. *Sci. Adv.* **5**, eaav6943 (2019).

Giant nonlinear damping in nanoscale ferromagnets

I. Barsukov, H. K. Lee, A. A. Jara, Y.-J. Chen, A. M. Gonçalves, C. Sha, J. A. Katine, R. E. Arias, B. A. Ivanov and I. N. Krivorotov

Sci Adv **5** (10), eaav6943.
DOI: 10.1126/sciadv.aav6943